Observation of Pipe Geometry with Progression of Backward Erosion Piping

Mitsu Okamura,[1] and Ryota Izawa,[2]

[1]Graduate School of Science and Engineering, Ehime University, 3 Bunkyo-cho, Matsuyama, Ehime Pref., 790-8577, Japan; e-mail: okamura@cee.ehime-u.ac.jp
Corresponding author.
[2] Graduate School of Science and Engineering, Ehime University, 3 Bunkyo-cho, Matsuyama, Ehime Pref., 790-8577, Japan; e-mail: g520025b@mails.cc.ehime-u.ac.jp

ABSTRACT

In order to better understand the mechanism of backward erosion piping, many experimental works has been conducted. Pipe geometry is a crucial parameter which have a direct effect on water flow and sand transportation in the pipe, and thus pipe progression. However, the measurement was available only after the tests, when model levees were removed. Evolution of the 3D geometry as the progression in pipe length has not been observed. This paper describes a newly developed innovative technique to measure 3D pipe geometry below levees. The technique is applied to centrifuge tests of backward erosion piping experiments and successfully obtained the evolution of pipe geometry as the pipe length progressed. Both width and depth of the pipe increased gradually with increasing the pipe length and significantly changed as soon as the pipe tip reached river water to form a direct connection.

INTRODUCTION

Backward erosion piping is an important failure mechanism for less-permeable river levees founded on sandy aquifers. The piping initiates in the form of concentrated leaks at the landside soil surface when the hydraulic loads generated by seepage exceed the capacity of the soil to resist. Shallow pipes are formed at the surface of the sandy aquifer by the erosion of sand particles, beginning at the landside ejection holes and progressively extending towards the riverside. The erosion process continues while the river water level is high enough; eventually, the pipe forms a direct connection between the landside and riverside, which accelerates the widening and deepening of the pipe, resulting in levee collapse and breach (ICOLD, 2015).

Many small-scale tests have been conducted in the investigation of backward erosion piping, which is a complex mechanism of water flow coupled with sand erosion and transportation. The pipe geometry and flow velocity were explored at the time when the sand in the pipe began to be transported, extending the pipe. Flow hydraulics and the criteria for pipe progression have been discussed which provided a basis for the development of a prediction method for backward erosion piping (e.g. Sellmeijer, 1988). Pipe geometry is a crucial parameter which have a direct effect on water flow and sand transportation in the pipe, and thus hydraulic gradient for pipe progression. Attempts have been made to measure 3D pipe geometry in model tests (e.g. van Beek et al., 2015;

Vandenboer et al., 2017; Okamura et al., 2022) but the measurement were available only after the tests, when model levees were removed. Evolution of the 3D geometry as the progression in pipe length has not been observed. In this study a new innovative technique has been developed which can measure 3D geometry of sand bed surface below model levees without removing the levees. This paper describes 3D pipe geometry in a centrifuge test using the technique at several pipe lengths. Evolution of pipe shape as extending the pipe length is discussed.

CENTRIFUGE TEST

Model preparation. The models were constructed in a rigid container with the internal dimensions of 530 mm in length, 120 mm in width, and 230 mm in height. Figure 1 illustrates the model configuration comprising a uniform medium dense sand bed with pervious and impervious retaining walls on the riverside (upstream) and landside (downstream), respectively, and a model levee resting on the bed. A clean silica sand, Keisa #5, was used of which grain size distributions and physical properties are shown in Figure 2. Dry sand was air-pluviated in the container to a depth of 60 mm at a target relative density of D_r = 60 %. After the surface of the sand bed was carefully levelled using a vacuum device, the model levee was placed on the sand bed. The model levee, with a length of L = 190 mm, was fabricated by the gluing of acrylic plates (10 mm thick), which were transparent for observing the pipes developing on the surface of the sand bed. To prevent the model levee from sliding on the bed during the flooding experiment, a weight was placed on the levee so that the total mass of the model levee would be equivalent to soil levee.

A high-speed camera was placed on the levee to closely observe the movement of the sand through the transparent base plate. A line laser and the camera were set to an angle which is capable to move laterally on linear ways.

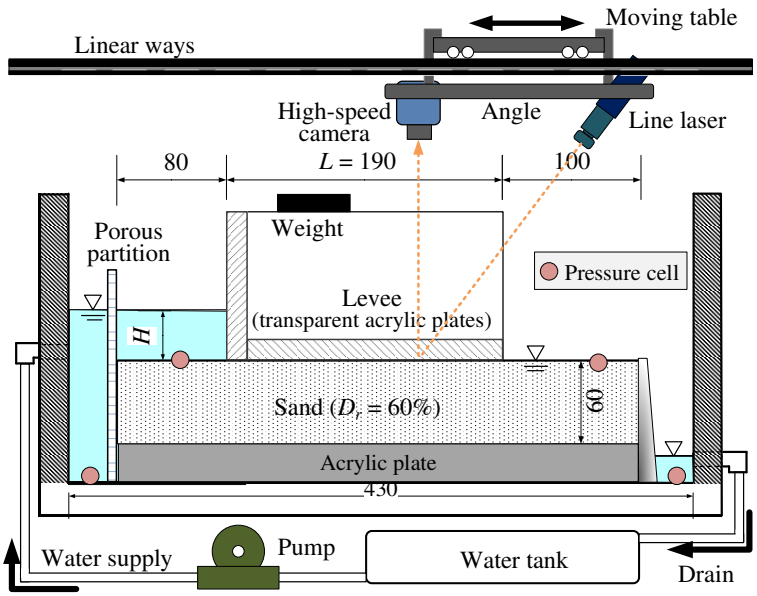

Figure 1. Test setup (all dimensions are in mm).

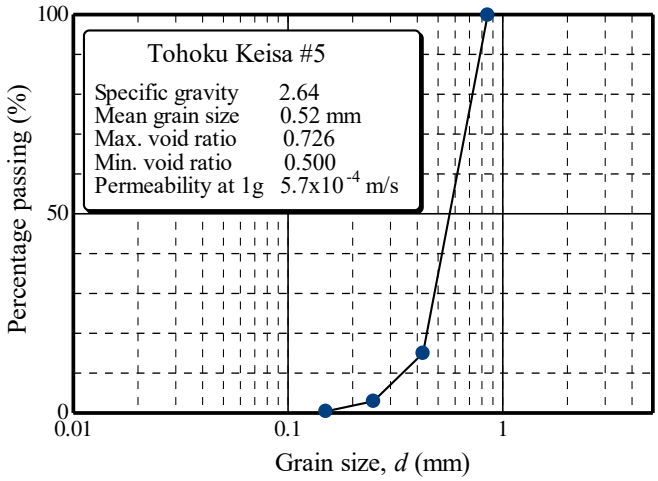

Figure 2. Grain size and physical properties of sand used in the tests.

Test procedure. Tests were conducted using a 20 g-ton beam centrifuge at Ehime University. The model was set on the centrifuge platform and spun to 40 g. Water was supplied by a pump to saturate the sand bed prior to flooding events. An advantage of using centrifuge in the saturation process is that a high degree of saturation can be achieved by introducing water to the sand bed at high-g environment (Okamura and Inoue, 2012). Moreover, heaving of the sand bed that might occur during the saturation process can be effectively avoided. The permeability coefficient in the centrifuge was 40 times higher than that obtained from laboratory tests indicated in Figure 1.

At 40g, the upstream water head (H) was controlled, whereas the water table was maintained constant at the sand surface on the downstream side, giving rise to the head difference across the levee, H. The line laser and camera on the linear ways were horizontally moved from the riverside toe to the landside toe to capture photos of irradiated laser lines at the sand surface over the area below the levee. The upstream water head was increased gradually as shown in Figure 4 until a pipe initiated with sand ejecta at the toe of the levee. The head was lowered once and increased stepwise again until the pipe length was extended to a few centimeters. This cycle of head changing was repeated until the pipe finally went through to the riverside. During the intervals of each step, the angle was moved to capturer photos of the laser lines.

Finally, the water was fully drained, the model levee was removed, and the digital elevation model of the pipe was obtained using the photogrammetric range imaging technique (SfM). The geometry at the end of test obtained with two different methods, the laser line technique and the SfM are compared to verify the validity of the line laser technique.

3D Pipe geometry measurement using line laser. Okamura et al. (2022) used laser scanner and SfM in centrifuge tests to obtain surface settlements and pipe geometry over an area. Providing accurate and detailed 3D surface geometry of models, they are available only after removing the model levee. Shinha et al. (2021) developed a new innovative method to measure a continuous settlement distribution along a laser line. The method uses line lasers and a camera to record the

projected laser lines on the model surface. They introduced the theory for converting horizontal movements of laser lines in pixel movements in photos to real surface settlement. In the present study, the method is extended further from measuring settlement on a line to the whole area of the model below the levee. This innovative technique developed in this study make it possible to observe 3D pipe geometry without removing the mode levee.

The device used in this study was 660 nm, 40 mW red light line laser produced by Kiko Giken Co. A cylindrical clamp attached to an angle was used to hold the lasers in place (see Figure 1). The hole on the angle were made to orient the laser at the angle $\theta_{in} = 30°$. A high-speed camera with 2448 px × 2048 px resolution was also set on the angle with its center facing vertically down at the laser line projected at soil surface. The angle was mounted on a moving table on linear ways which equips a position transducer to determine the precise location of the camera.

Figure 3 is schematic diagrams showing the change in the location of a laser line for settlement of sand bed surface. Depth of the water saturated pipe is expressed as,

$$\Delta v = \Delta u \tan\theta_l \tag{1}$$

where θ_l is an angle of refraction depending on the refraction indices of air (n_{air}) and water (n_{water}). Δu is the horizontal distance of laser lines obtained by comparing a set of two photo images which are captured for the same camera location, X, before and after the sand surface settlement due to the formation of pipes. The captured photo images are processed to obtain horizontal movements the laser line in pixels (Δpx in x-direction) along the line in y-direction. The camera is initially calibrated to correct the photos to obtain the calibration factor (f_{px-mm}). The calibration factor is the extrinsic property representing the number of pixels per unit millimeter of the physical measurement of real-world objects in the image. In the experiment the calibration factor f_{px-mm} was determined as 17.2 px/mm. The horizontal movement is given as $\Delta u = \Delta px / f_{px-mm}$. Distribution of pipe depth along with a laser line is obtained.

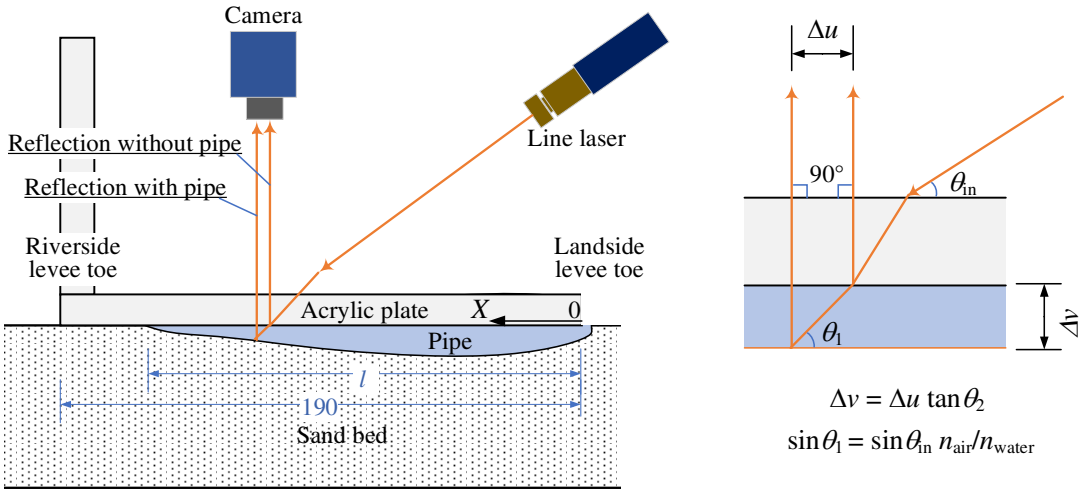

Figure 3. Change in location of laser lines captured by the camera (Δu) due to settlement of sand bed surface (Δv) under the acrylic levee.

The angle with the camera and line laser was moved laterally at the constant rate of 15 mm/s so that the laser was irradiated whole area of the sand bed surface beneath the levee, from X = 0 (landside toe) to 190 mm (riverside toe). Photo images of laser lines were captured at a constant rate of 30 frame/s. The images of laser lines are obtained at an interval of 0.5 mm in X-direction. Figure 4 shows a position of photo relative to the levee base with coordinates x-y in pixel and X-Y in mm set to the photos and levee base, respectively. The laser line position in this figure was initially x = 700 px as indicated by the broken line and slightly moved leftward as the sand surface subsided. The shape of pipe sections was analyzed every 5 mm along with X-coordinate.

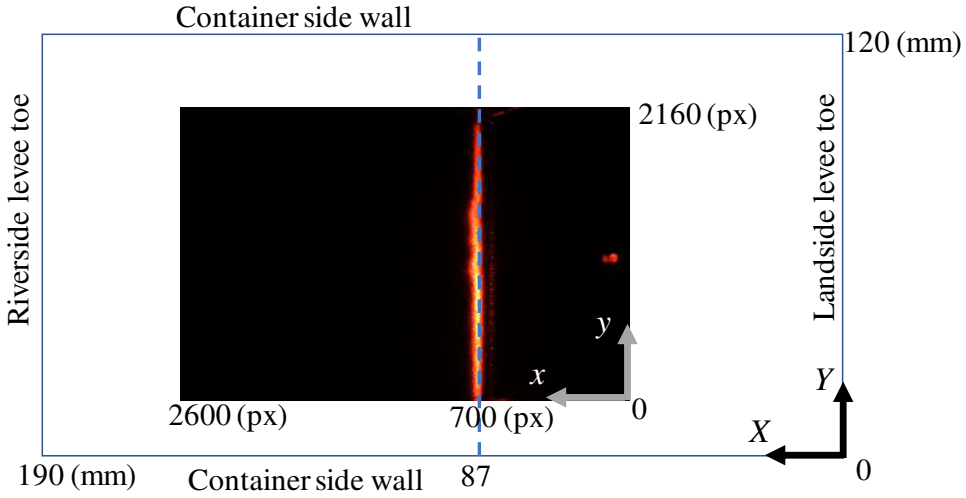

Figure 4. Plan view of levee base and a photo of a laser line at X= 87 (mm) (not to scale).

RESULTS AND DISCUSSIONS

Hydraulic Gradient for pipe progression. The time histories of hydraulic gradient (H/L) and normalized length of pipe (l/L) in the test are shown in Figure 5. Here, l does not indicate the actual meandering pipe length; it represents the distance from the pipe tip to the levee toe. Sand ejected at toe and piping initiated at H/L = 0.22 (t = 320 s). In the next step the pipe developed to l/L = 0.26 at slightly lower gradient of H/L= 0.205 and stabilized thereafter. The pipe extended at approximately same gradient until l/L reached 0.53 in 3rd and 4th steps followed by a quick progression at gradient lower than 0.2 in 5th step. The progression gradient (H/L) remains nearly constant for l/L= 0–0.5, and thereafter, decreases with the increase in l/L. Many previous experiments reported in the literatures employed a small exit hole in the landside, which ensured pipe initiation at a relatively low head and the pipe equilibrium was likely to occur. In those experiments, equilibrium in pipe development was observed after the initiation and the increase in H is required to make the pipe progress until the critical head is reached. The test in this paper may be classified as "Initiation dominated test" (Bonelli, 2011).

In the last step the riverside water head was started to decrease when the l/L reached at approximately 0.8 but the pipe extension was so fast that the pipe tip reached the riverside toe.

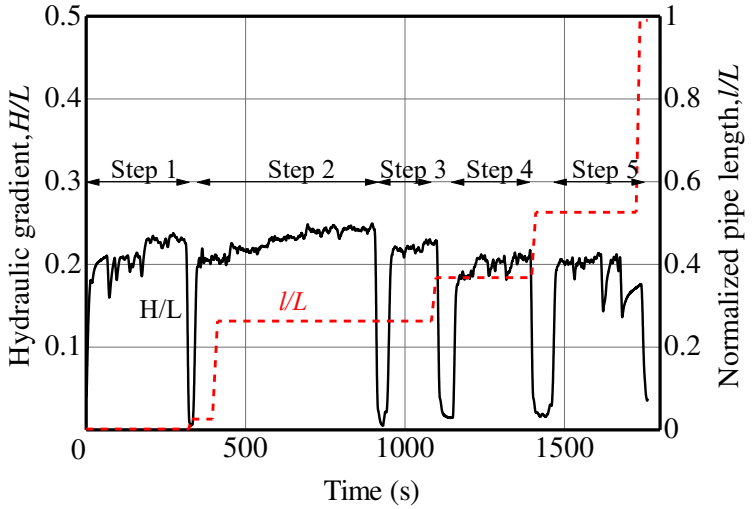

Figure 5. Time histories of hydraulic gradient and normalized length of the pipe.

Image processing for pipe geometry measurement. Figure 6(a) shows a captured image of a laser line at distance from toe X = 140 mm after step 5. Distributions of luminance values on y = 1092 px are depicted in Figure 6(b) where the luminance distribution of the same location before the 1st step is also shown for comparison. The center of gravity of the distributions and hence the laser points' coordinates are identified as shown by the arrows in the figure. Although the high-quality laser with sharper line width of 0.3 mm was used, the width of laser line became considerably wider due to the scattering at the surface of acrylic plate. For each y-coordinate, scanning was done to identify the change in the laser positions from that before Step 1, Δpx.

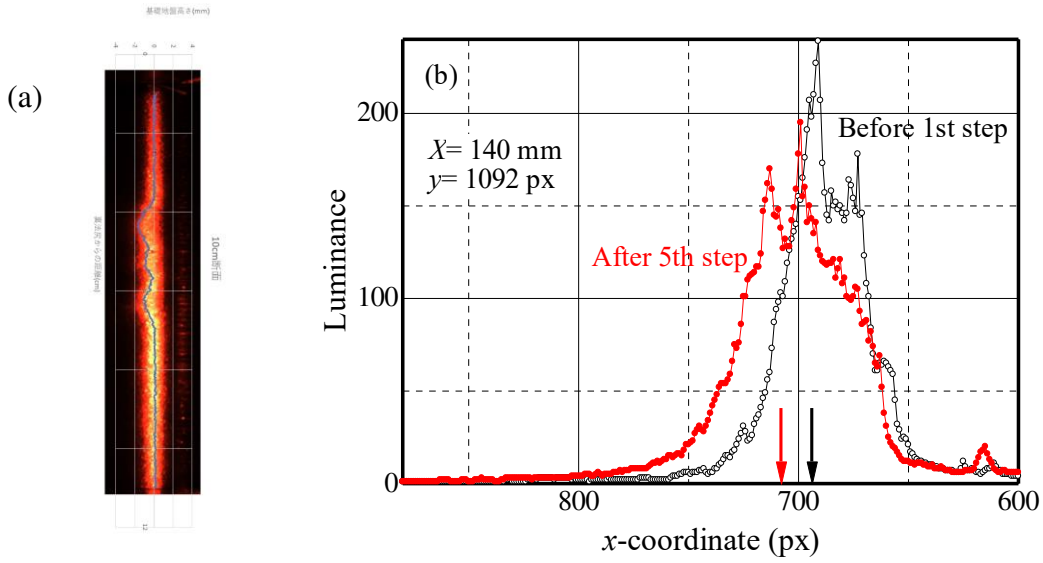

Figure 6. (a) Captured images of a laser line at 140 mm from the levee toe captured after the test. (b) luminance distribution along x-coordinates at Y = 77 mm.

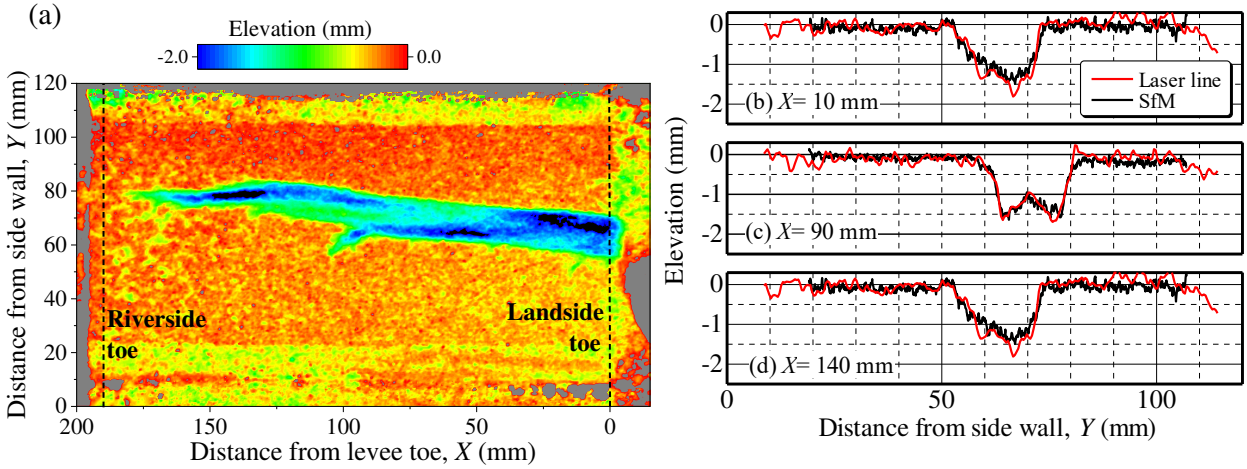

Figure 7. Elevation of sand bed surface and cross sections of the pipe after the test. (a) Surface elevation obtained by SfM after removal of the model levee, (b)-(d) comparisons of pipe cross section after the test obtained by two different methods.

After the test, model levee was removed and the surface of sand bed was photographed from variety of angles to establish 3-D DEM. Figure 7(a) shows the elevation of the sand where the pipe can be clearly seen. The pipe developed in a linear manner with a small branching appeared at $X = 95$ mm. Just before the removal of the levee, the sand surface below the levee was also measured with the line laser technique. Cross-sections of the sand bed surface obtained by the two methods are compared in Figure 7(b). The geometry of the piping channel obtained by the line laser technique agrees quite well with those by SfM, verifying the validity of the technique newly developed in this study. The pipe cross sections were generally U shape with an exception for $X =$ 90 mm where the pipe branched and two channels appeared. Typical depth of the pipe ranged from1.5 to 2.0 mm, which is approximately three to four times the mean sand grain diameter.

Change in Geometry with Progression of pipe. Figure 8(a) illustrates plan view of the pipe observed at the end of each step. A pipe initiated from the levee toe extended towards riverside and the width of the pipe increased with the pipe length. Pipe cross sections at four locations, $X =$ 25, 50, 75 and 90 mm, are shown in Figure 8(b)-(e). Near the exit ($X = 25$ mm), the pipe tip passed in the second step and both depth and width slightly increased at the end of 3rd and 4th step with the general shape keeping almost constant. It is also the case at $X = 50$ mm where the pipe tip passed in the 3rd step and the pipe cross section at the end of 3rd and 4th are quite similar in shape but slightly wider for the latter step. After 5th step in which the direct connection established and larger amount of water flowed through the pipe, cross sectional shape significantly changed. Width of pipe increased significantly while the depth did not.

As the pipe length increased, water catchment zone in the sand bed expanded resulting in the increase in amount of water flowed in the pipe. Being constrained by the critical Shields number (Okamura et al., 2022), water flow condition in the pipe with the increased flow rate may

be balanced by the expansion of the section. Figure 9 shows the pipe cross-sections that are converted to circular pipes with equivalent diameter as,

$$D_e = 4A / P \tag{2}$$

where A and P denote the cross-sectional area and wetted perimeter of the pipe, respectively. D_e increases very gradually with the distance from the pipe exit for the range $0 < X < l/2$. While for the range near the tip, $3l/4 < X < l$, D_e increases sharply with the distance from the tip. This may be explained by facts that the pressure difference in the pipe and adjacent sand bed is largest at the rip and decreases with distance from the tip, and water inflow is likewise. In order to accommodate water flow in the pipe, pipe sectional area increased sharply near the tip and very gradually near the exit.

For any steps, pile equipment diameter decreases towards the tip, with D_e being larger for longer pipe. This may suggest that D_e would be larger for larger models. Despite D_e observed in the present study is only several times the sand grain size, much longer pipe in larger models and full scale levees which accommodate larger amount of water flow is considered to have larger D_e. Scale effects of pipe size as well as critical hydraulic gradient is indeed a topic which needs further study.

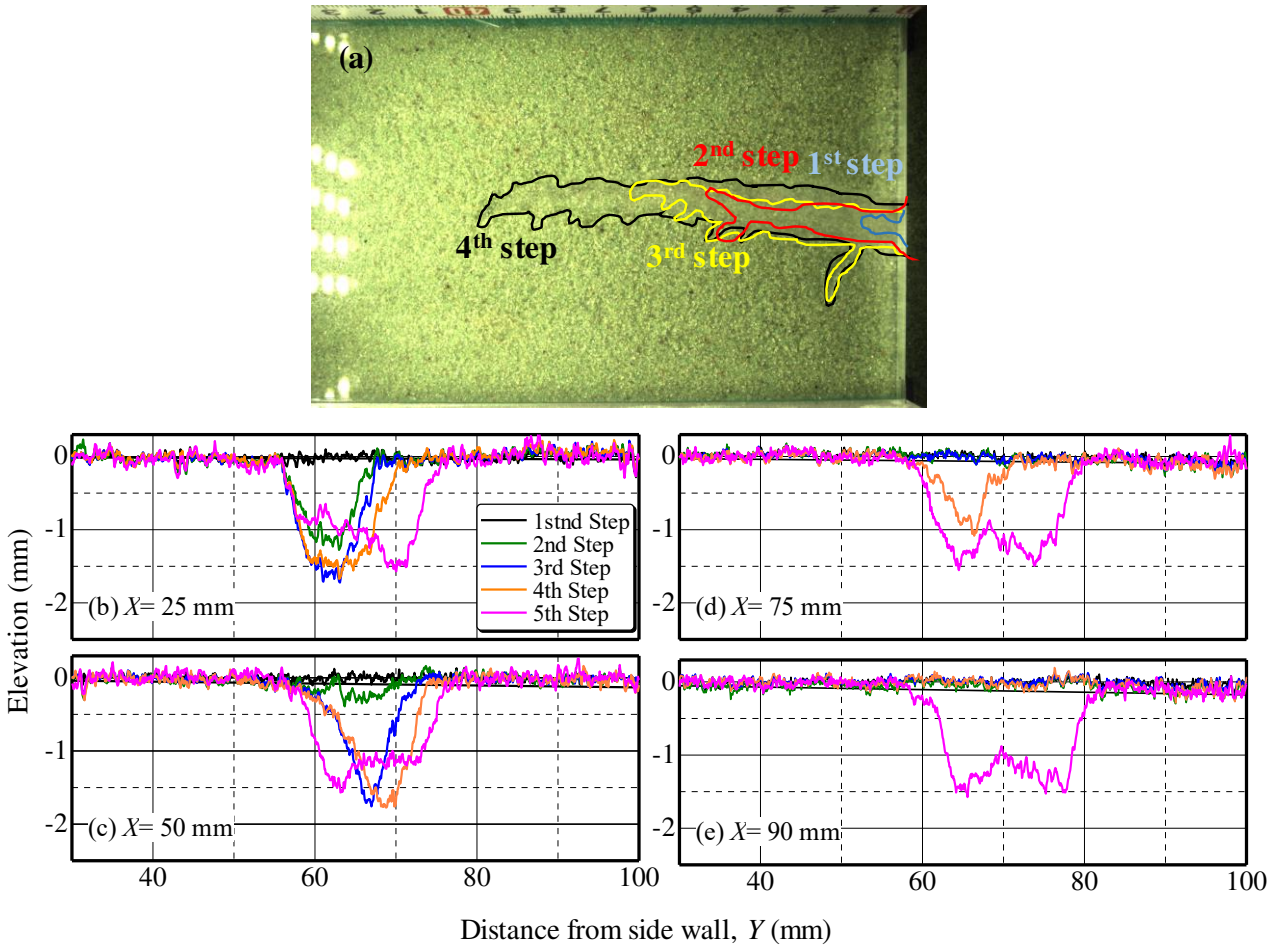

Figure 8. Piping at the end of steps. (a) Plan view, (b)-(e) Selected pipe cross sections.

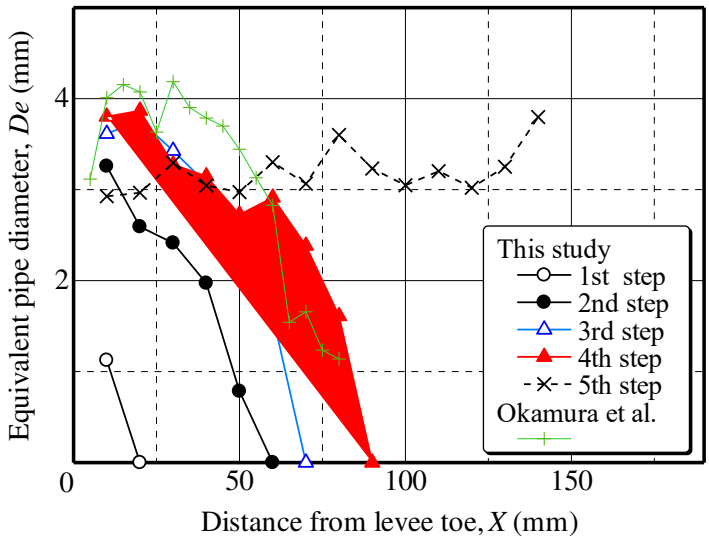

Figure 9. Evolution of equivalent pipe diameter along the length for four steps.

CONCLUSION

This paper describes a newly developed innovative technique to measure 3D pipe geometry below transparent model levees. A set of a line laser and a camera installed on linear ways was used and subsidence of sand surface blow the transparent levee was estimated from distances of laser lines captured in two photos taken before and after test.

The technique is applied to the centrifuge test on backward erosion piping. In the test, the head difference changed in steps so that the piping developed gradually until the pipe tip reached the riverside to form direct connection between river water and the exit of the pipe at the landside levee toe. In each step, the irradiated laser lines to the sand bed surface were captured by the camera over the area below the levee. After the test, the model levee was removed to expose the sand bed surface and the geometry of the pipe was obtained using SfM (structure for motion). The geometry of sand bed surface at the end of the test obtained by the two methods, the line laser method and SfM, agreed reasonably well, confirming the validity of the newly developed technique.

The analysis of pipe geometry in all steps clearly indicates the evolution of pipe geometry as the pipe length progressed; both width and depth of the pipe increased gradually with increasing the pipe length. Cross sections of the pipe changed significantly after the direct connection established.

REFERENCES

Bonelli, S., ed. (2013). *Erosion in geomechanics applied to dams and levees*. Hoboken, NJ: Wiley.

ICOLD. (2015). *Internal erosion of existing dams, levees and dikes, and their foundations.* ICOLD Bulletin 164.

Okamura, M. and Inoue, T. (2012). "Preparation of fully saturated models for liquefaction study. "*Int. J. of Physical Modelling in Geotechnics*, 12 (1), 39–46.

Okamura, M., Tsuyuguchi, Y., Izumi, N. and Maeda, K. (2022). "Centrifuge modeling of scale effect on hydraulic gradient of backward erosion piping in uniform aquifer under river levees. "*Soils and Foundations*, 62(5), 101214.

Sinha, S.K., Kutter, B.L. and Ziotopoulou, K. (2021). "Measuring vertical displacement using laser lines and cameras. "*Int. J. Physical Modelling in Geotechnics*, 23(1), 3–15.

Van Beek, V. M., Van Essen, H. M., Vandenboer, K.and Bezuijen, A. (2015). "Developments in modelling of backward erosion piping."*Géotechnique* 65(9), 740–754.

Vandenboer, V., van Beek, V. M. and Bezuijen, A. (2017). "Pipe depth measurement in small-scale backward erosion piping experiments. "*Proc. 25th Meeting of the European Working Group on Internal Erosion*, 21-28.